Journal of Nonlinear Optical Physics & Materials
Vol. 18, No. 1 (2009) 49–72
© World Scientific Publishing Company

World Scientific
www.worldscientific.com

POLARIZATION COUPLING OF LIGHT WAVES IN PERIODICALLY POLED LITHIUM NIOBATE AND ITS APPLICATIONS

XIANFENG CHEN*, KUN LIU and JIANHONG SHI

Department of Physics, The State Key Laboratory on Fiber Optic Local Area Communication Networks and Advanced Optical Communication Systems Shanghai Jiao Tong University, 800 Dongchuan Rd. Shanghai 200240, China
**xfchen@sjtu.edu.cn*

Received 16 March 2009

In this paper, we review current research on the applications of periodically poled lithium niobate (PPLN) by use of polarization coupling in our and other research groups. Tunable wavelength Solc-type filter, polarization controller and electro-optical switch based on PPLN are presented, which show potential applications in optical communications and optical information processing.

Keywords: Polarization coupling; periodically domain inverted ferroelectric crystal; lithium niobate.

1. Introduction

Ferroelectric crystals are important materials in many kinds of applications. Since the invention of so called quasi-phase matching technique, periodically domain-inverted ferroelectrics crystals with modulated second order nonlinear susceptibility has received much attention owing to its outstanding nonlinear optical properties.[1–3] In periodically domain-inverted ferroelectrics crystals, besides the nonlinear optical coefficients, other third-rank tensors, such as the electro-optic (EO) coefficient, are also modulated periodically because of the periodically reversed ferroelectric domains. Since the theoretical research on EO effect in PPLN was proposed by Y. Q. Lu *et al.*,[4] this periodically modulation of the EO coefficient has given birth to some novel essential applications, especially when the voltage is applied along the transverse direction of the crystal. In this paper, current research of transverse EO-based PPLN applications, such as tunable wavelength filter, polarization controller, electro-optical switch and laser Q-switch in periodically poled lithium niobate are summarized.

2. Solc-Type Wavelength Filter

Tunable optical filters play an important role in optical signal processing and optical communication. In particular, a narrow flat-top bandpass filter, which not only enables a particular wavelength channel to pass through but is also significant to keep the signal stable, as well as a multiple-wavelength filter, which enables several wavelengths to pass through together at the same time, are widely needed in wavelength-division multiplexing systems. In this section, we present our research on tunable filter with single-wavelength, multiple-wavelength and flat-top passband based on PPLN crystal. Photovoltaic effect in PPLN is also investigated and based on which a tunable filter by use of UV light is demonstrated. Moreover, the latest researches on solc-type filter based on Ti:PPLN channel waveguide are also presented in the end of this section.

2.1. *Principles*

When an electric field is applied along the Y axis of a crystal with 3m symmetry, the new index ellipsoid deforms to make its principal axes rotated at an angle θ about the x axis with respect to the unperturbed principal axes. Since θ is proportional to the product of the electric field and the electro-optic coefficient, when an uniformed electric field applying along the Y axis of the crystal, the rotation angle of the original domain is opposite to that of the inverted domain because of the reversal of the spontaneous polarization.[4] Thus, in a periodically domain inverted crystal with a uniformed electric field applied along the Y axis, a structure with alternating left and right rotation angle θ will be formed due to the periodic EO coefficient. This structure is similar to the well-known folded Solc filter structure with alternating azimuth angles of the crystal axes. So we call it Solc layered structure.

To have an insight into the filter process, polarization coupled-mode theory is established to track the polarization state of light propagation along PPLN. In PPLN the coupled-wave equations of the ordinary and extraordinary waves are:

$$\begin{cases} dA_1/dx = -i\kappa A_2 \exp(i\Delta\beta x) \\ dA_2/dx = -i\kappa^* A_1 \exp(-i\Delta\beta x) \end{cases} \tag{1}$$

with $\Delta\beta = (k_2 - k_1) - G_m$, $G_m = 2\pi m/\Lambda$ and $\kappa = -(\omega/2c)(n_o^2 n_e^2 \gamma_{51} E_y/\sqrt{n_o n_e})$ $(i(1-\cos m\pi)/m\pi)$ $(m = 1, 3, 5, \ldots,)$, where A_1 and A_2 are the normalized amplitudes of the ordinary wave and the extraordinary wave, respectively, k_1 and k_2 are the corresponding wave vectors, G_m is the mth reciprocal vector corresponding to the periodicity of poling. Consider an input light with Y-axis polarization direction, the boundary condition of the equation is given by

$$\begin{cases} A_1(0) = 1 \\ A_2(0) = 0 \end{cases} \tag{2}$$

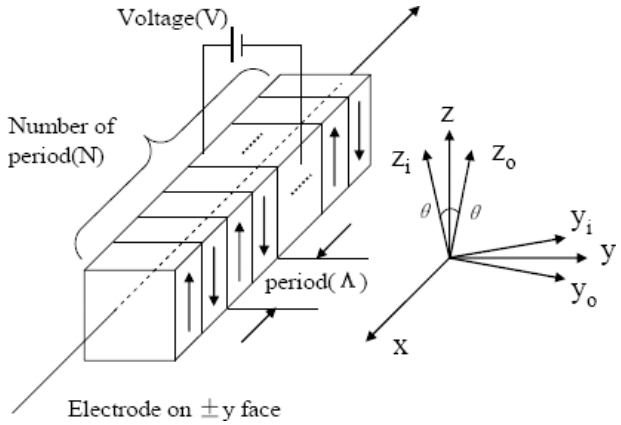

Fig. 1. Schematic diagram of a Solc layered structure based on electro-optic periodically domain inverted crystals. X, Y and Z are the principal axes of the unperturbed index ellipsoid. Λ is the period of this structure and N is the period number. The arrows inside the structure indicate the spontaneous polarization directions. Y_O, Z_O and Y_i, Z_i are the new perturbed principal axes of the original domains and the inverted domains with external electric field, respectively.[4]

So the solution of coupled-mode equation (1) is:

$$\begin{cases} A_1(x) = \exp[i(\Delta\beta/2)x][\cos sx - i(\Delta\beta/2s)\sin sx] \\ A_2(x) = \exp[-i(\Delta\beta/2)x](-i\kappa^*)\sin sx/s \end{cases} \tag{3}$$

where s is given by $s^2 = \kappa\kappa^* + (\Delta\beta/2)^2$.

When $\Delta\beta = (k_2 - k_1) - G_m = 0$, the reciprocal vector compensates for the wave-vector mismatch. We call this condition a QPM polarization conversion condition, which determines the fundamental wavelength of this kind filter. Under QPM condition, the transmission along the Z-axis is given by

$$T = |A_2(x)/A_1(0)|^2 = \sin^2(Sx) \tag{4}$$

If $|Sx| = |\kappa|L = (2m+1)\pi/2$, $(m = 0, 1, 2, \ldots,)$, then $T = 100\%$ and the power of the input light is completely transferred from Y polarization to Z polarization. Thereby, with a polarizer along Z-axis at the output, the fundamental wavelength will pass it without any loss, while at the same time wavelengths which do not satisfy this condition will be forbidden by the analyzer. The working mechanism of solc-type filter can also be easily understood as follows: because each domain serves as a half-wave plate with respect to the fundamental wavelength. After passing through the stack of half-wave plates, the optical plane of polarization of the fundamental wavelength rotates continually and finally emerges at an angle of $2N\theta$, where N is the number of plates. Therefore, when $2N\theta = 90^\circ$ at the filter output, light of the fundamental wavelength does not experience loss in passing through the crossed analyzer.

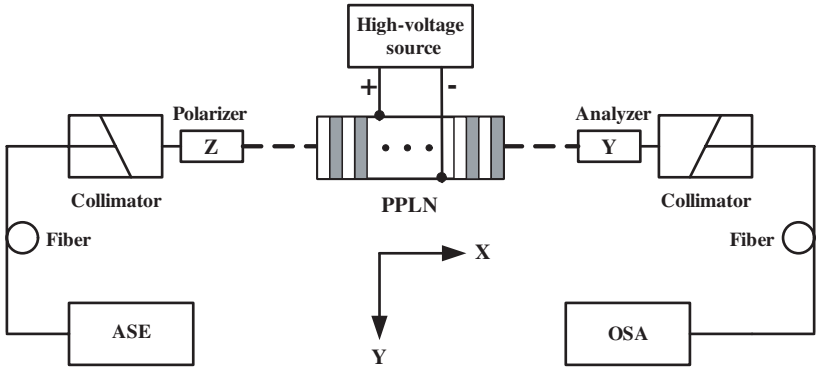

Fig. 2. Experimental setup for a PPLN single-wavelength filter. A PPLN crystal, which is Z cut, is placed between two crossed polarizer, the first of which is along Z direction and the second Y direction. The light propagates along the X direction and a uniform electric field is applied along the Y axis of the PPLN sample. ASE, amplified spontaneous emission; OSA, optical spectrum analyzer.[5]

2.2. *Device of tunable Solc-type wavelength filter*

2.2.1. *Tunable single-wavelength filter*

The first observation of a Solc filter based on PPLN operating in the optical communication wavelength range was proposed by our group in 2003.[5] Similar to the traditional folded type Solc filter, a PPLN crystal is placed between two crossed polarizer. This sample is with dimensions of 28 mm × 5 mm × 0.5 mm consisting of four gratings with periods from 20.2 to 20.8 μm and a width of 1 mm. A measured transmission power versus wavelength for 20.6 μm and 20.8 μm period is shown in Fig. 3, from which a typical transmission spectrum of traditional Solc-type filter can be seen. The amplitude modulation of the transmission power by applying an electric voltage along the Y axis of the PPLN is also observed and the result is shown in Fig. 4. In the above discussion, we have known that the fundamental wavelength is determined by equation $\Delta\beta = (k_2 - k_1) - G_m = 0$, which can be simplified to $\lambda_0 = \Lambda(n_o - n_e)$. Because the refractive indices of the ordinary wave and the extraordinary wave are temperature dependent, yet the fundamental wavelength can be shifted to a series of different wavelengths by changing the temperature. The experiment result on wavelength modulation is shown in Fig. 5, where $-0.415\,\text{nm}/^\circ\text{C}$ tuning rate is achieved. Wavelength tuning by temperature is interesting in dense wavelength division multiplexer optical fiber communication systems, where it can be employed as a wavelength-tunable filter for all-optical wavelength routing.

2.2.2. *Tunable multiple-wavelength filter*

In the previous section, we have discussed that the central wavelength of a PPLN Solc-type filter is determined by the period of the domain inversion and the ordinary

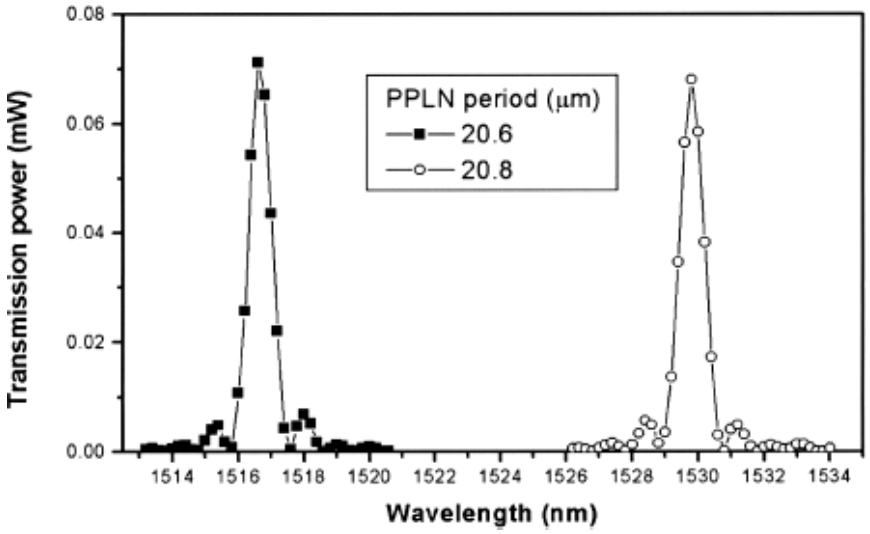

Fig. 3. Measured transmission power versus wavelength of the Solc filter in the 20.6- and 20.8-mm-period PPLN at a temperature of 24°C. The FWHM of the transmission spectrum is ~ 0.8 nm.[5]

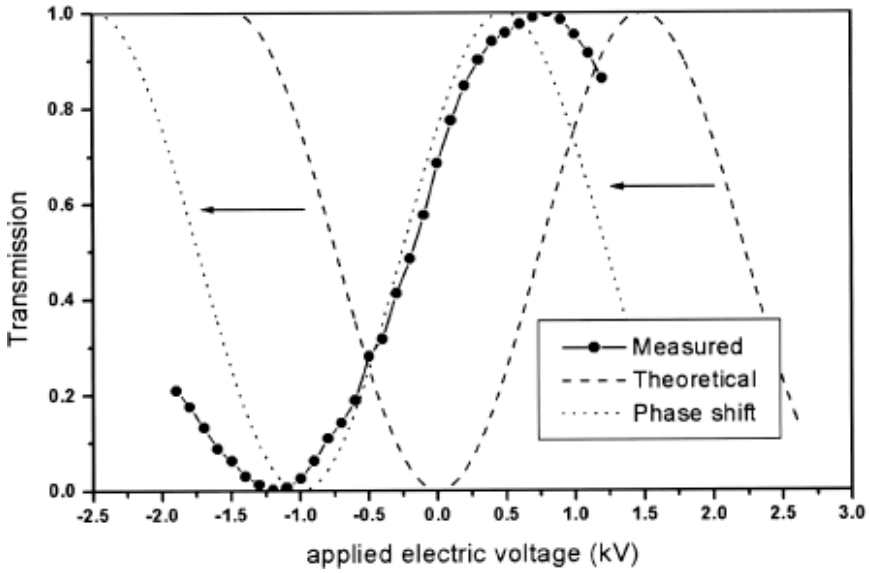

Fig. 4. Experimental measurement of the normalized transmission of the Solc filter (20.8 mm) as a function of the applied voltage at 24°C for a given wavelength of 1529.80 nm. The solid curve is the experimental measurement, the dashed curve represents the theoretical values calculated from the Sellmeier equation,[6] and the dotted curve is phase shifted from the dashed curve for comparison with the experiment.[5]

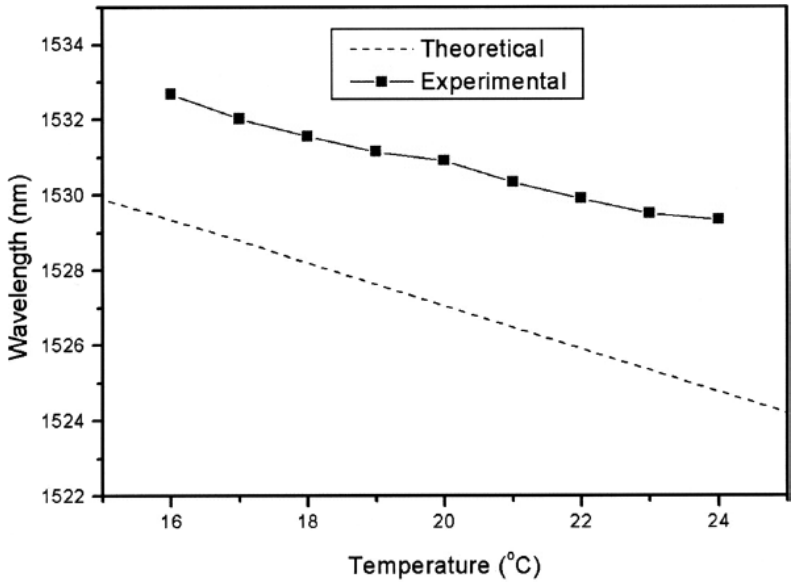

Fig. 5. Experimental measurement of the central wavelength of the Solc filter (20.8 mm) as a function of the temperature without the applied external electric voltage. The dashed line represents the theoretical values calculated from the Sellmeier equation from Ref. 6, and the solid curve is the experimental measurement.[7]

and extraordinary refractive indices. Since the indices are temperature dependent, the central wavelength of such filter can be shifted by changing the working temperature of the whole PPLN. If we apply a temperature distribution along the PPLN through a local-temperature-control technique to control and reshape the second harmonic (SH) curve, then the PPLN will be divided into several temperature sections and each section will give a central wavelength determined by its local temperature. By combining the contributions from all the temperature sections in the PPLN, a multi-wavelength filter can be realized. By properly controlling the temperature of each section, we can construct a tunable multi-wavelength filter for any wavelength according to the practical needs of different applications.[8]

The multiple-wavelength filter can also been designed by optimizing the sequences of the opposite domains in aperiodic poled lithium niobate (APLN) using simulated annealing (SA) algorithm.[9] Here, Jones matrix, a 2×2-matrix method, is employed to track the polarization state of light propagation along APLN.[10] The sequence of the positive and negative domains is optimized with the target that the transmission of the prescribed wavelengths are equal with maximum values at the same time. Here, we chose the objective function in the SA method as

$$F = \sum_{\alpha} T(\lambda_\alpha) - \{\max[T(\lambda_\alpha)] - \min[T(\lambda_\alpha)]\} \tag{5}$$

where the symbol $\max[\cdots]$ ($\min[\cdots]$) manifests to take their maximum (minimum) value along all the quantities including into $[\cdots]$. λ_α is the transmission wavelength

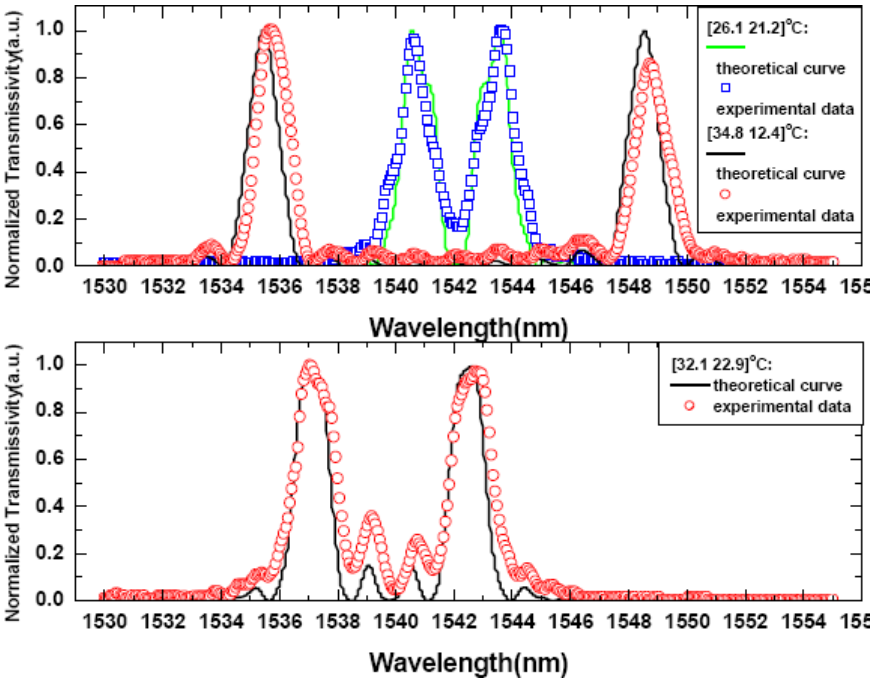

Fig. 6. Tunable double-wavelength filter realized in PPLN by applying a two-section pattern temperature distribution along the sample. In the first figure, under a [26.1 21.2]°C pattern temperature distribution, the double peaks were at 1540.616 nm and 1543.63 nm, and under a [34.8 12.4]°C pattern temperature distribution, the double peaks were tuned to 1538.562 nm and 1545.6845 nm, for the symmetrical case. In the second figure, under a [32.1 22.9]°C pattern temperature distribution, the double peaks were set to 1537.078 nm and 1542.763 nm, for the arbitrary case.[8]

selected as the objective wavelength in the function. In our calculation, the length of each domain is set to be 5 μm. The length L of lithium niobate is 5 cm and the number of blocks is $N = 10000$. The wavelength dependent refractive indices of extraordinary wave and ordinary wave are calculated at 20°C from the Sellmeier equation.[6] Wavelengths 1548.5, 1550.1, 1551.7, and 1553.3 nm are chosen as the filtering wavelengths of APLN filter. These wavelengths are from ITU standard wavelength table for DWDM optical communication, with frequency spacing of 200 GHz. Figure 7 shows the filtering results of two, three and four 200-GHz-spaced DWDM wavelengths by simulated annealing algorithm.

The first experimental observation of narrowband multi-wavelength filters based on aperiodically poled lithium niobate crystals was reported by Lin *et al.*[11] In the experiment, they simultaneously transmitted 8 ITU-standard wavelengths through a 5-cm long EO APLN filter with a transmittance of >90% and a bandwidth of ~ 0.45 nm for each wavelength channel. Moreover, the transmission spectrum of the EO APLN filter can be conveniently tuned by temperature at a rate of ~ 0.65 nm/°C in the telecom C band.

2.2.3. *Flat-top wavelength filter*

Generally, the passband of this kind filter is extremely narrow. Tiny shift of the fundamental wavelength because of unstable temperature or any other factors will contribute to great loss. Thereby, a flat-top filter which can avoid the interference of the outside and maintain signal quality is necessary.

To begin with this section, we would like to introduce the spectrum waveform similarity (SWS) rule discovered in PPLN firstly.[12] The SWS rule can be described as follows: if the product of the domain N and the rocking angle θ is fixed, the shape

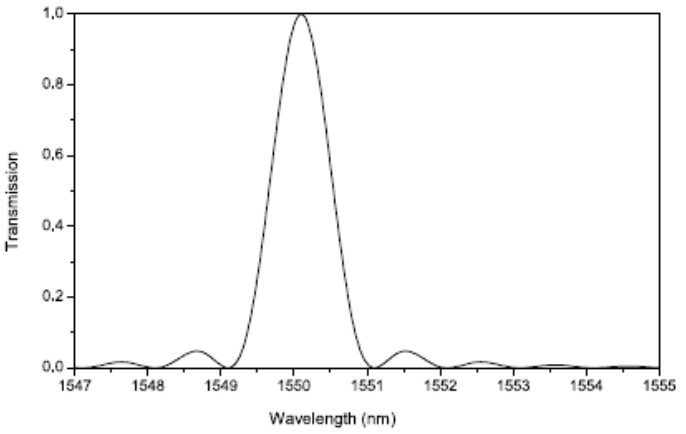

(a)

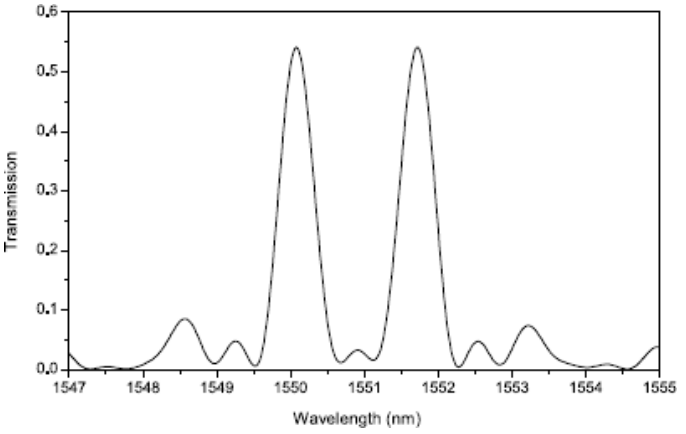

(b)

Fig. 7. Calculated transmission spectra of narrowband multiple wavelengths filters at 20°C. The length L of lithium niobate is 5 cm. (a) A spectrum of PPLN Solc filter. (b)–(d) Transmission spectrums with two, three and four peaks in APLN filters optimized by SA method. The number of domains is $N = 10000$ and the applied electric field in Y-direction is 70 V/mm. The peak wavelengths are 1548.5, 1550.1, 1551.7 and 1553.3 nm, respectively.[9]

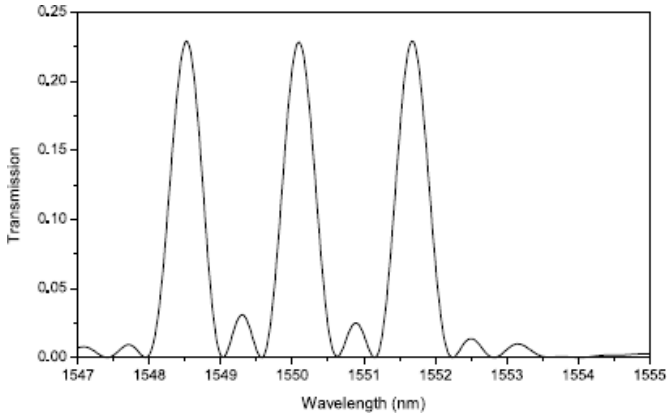

(c)

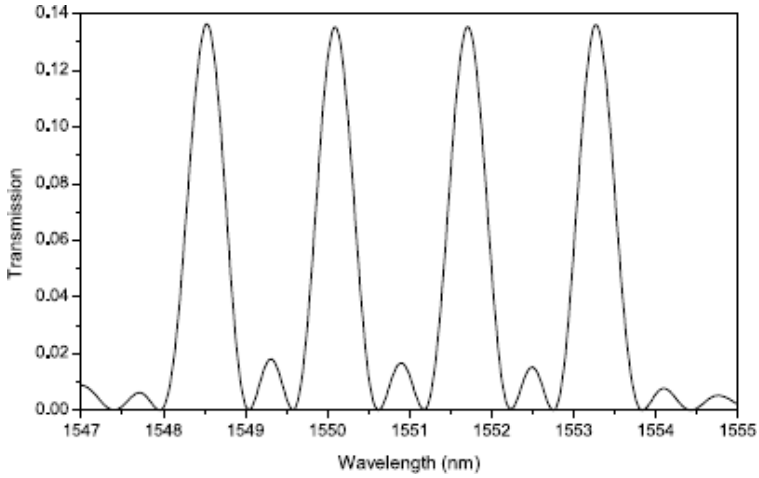

(d)

Fig. 7. (*Continued*)

of the spectrum waveform remains similar, as N varies. To get a clear picture of this rule, Fig. 9 will be helpful. In Fig. 9, "A" represents the product of the domain N and the rocking angle θ. With "A" fixed at $\pi/2$, the shape of the spectrum waveform remains similar when N is changing, despite the FWHM correspondingly increases. Based on the spectrum waveform similarity (SWS) rule, we come to a conclusion that the shape of the spectrum waveform is determined by the product A. By observing the spectrums at different value of A, our study reveals a critical point ($A = 2.24$) at which the spectrum surprisingly evolved into flat-top type (Fig. 10). The 1 dB width of the flat-top waveform can be fitted as follows

$$\Delta\lambda_{1db} \approx 2.5\lambda_0/N \tag{6}$$

where λ_0 is the fundamental wavelength of the filter.

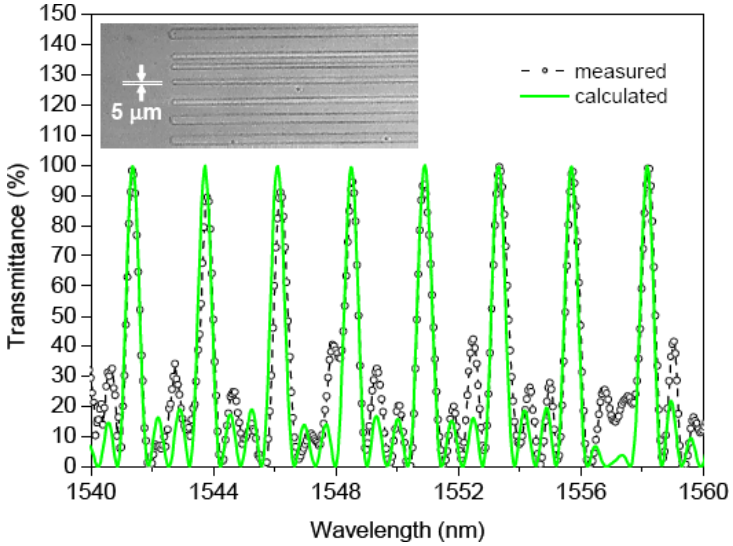

Fig. 8. Calculated (solid line) and measured (open circles) transmission spectra of the 5-cm long EO APLN filter. The two spectral curves agree reasonably well, except that the side lobes in the experimental curve are more apparent. The inset shows a microscopic image of an HF-etched z surface of the fabricated APLN crystal. The label in the inset indicates the width of the unit domain block used in this APLN crystal, i.e., $\Delta x = 5\,\mu$m.[11]

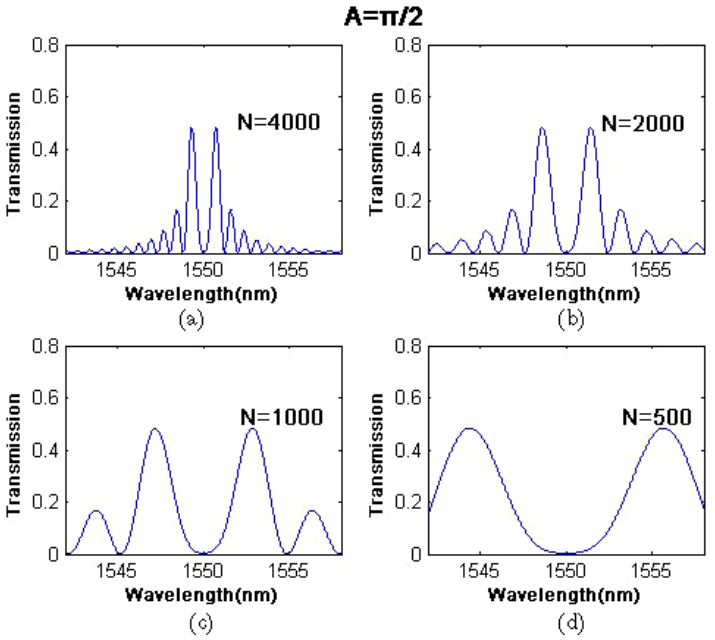

Fig. 9. The transmission spectrums by use of numeral calculation in PPLN with the product A fixed at $\pi/2$. (a) The transmission spectrum with N at 4000; (b) The transmission spectrum with N at 2000; (c) The transmission spectrum with N at 1000; (d) The transmission spectrum with N at 500.[12]

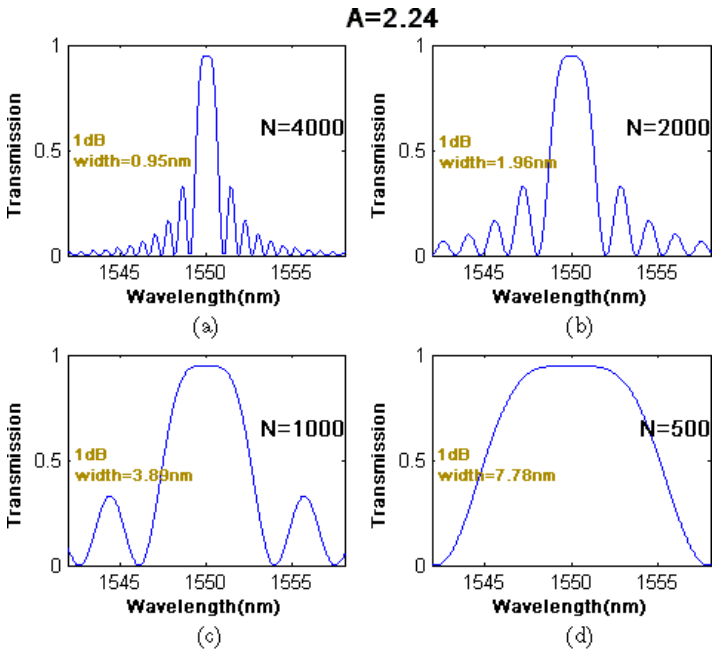

Fig. 10. The transmission spectrums by use of numeral calculation in PPLN with the product A fixed at 2.24. (a) The transmission spectrum with N at 4000; (b) The transmission spectrum with N at 2000; (c) The transmission spectrum with N at 1000; (d) The transmission spectrum with N at 500.[12]

In order to confirm this theoretical discovery about flat-top spectrum in PPLN, further investigation has been performed experimentally. The PPLN sample, employed in the experiment, with a dimension of $30(\mathrm{L}) \times 10(\mathrm{W}) \times 0.5(\mathrm{T})\,\mathrm{mm}^3$ consists of 2857 domains with the period of 21 (μm). In above discussion, we have known the flat-top spectrum requires $N\theta = 2.24$ which is greater than the single wavelength Solc-type filter ($2\mathrm{N}\theta = \pi/2$). Thereby, as to a given PPLN (N fixed), higher electric field is requested than usual. During the experiment, the transmission of the fundamental wavelength attends to maximum at 3 (kV/cm) (A) and gradually declines when the electric field keeps on arising subsequently. Consistent with the theoretical result, the spectrum evolves into flat-top type with higher electric field at the critical point 4.2 (kV/cm) (B). The corresponding transmission spectrums at A and B are, respectively, shown in Fig. 11. A flat-top waveform with 1 (nm) flat-top width is obtained in the experiment.

Interestingly, as to a given PPLN, by extending the external electric field to a higher value, the theoretical results reveal that new critical points of flat-top will be found every 2.4 (kV/cm) electric field. Besides, the width of each flat-top transmission spectrum is proportionally increased with the increment of external electric field. Thereby, tunable passband can be achieved by switching the external electric field between different critical points which is shown in Fig. 12.

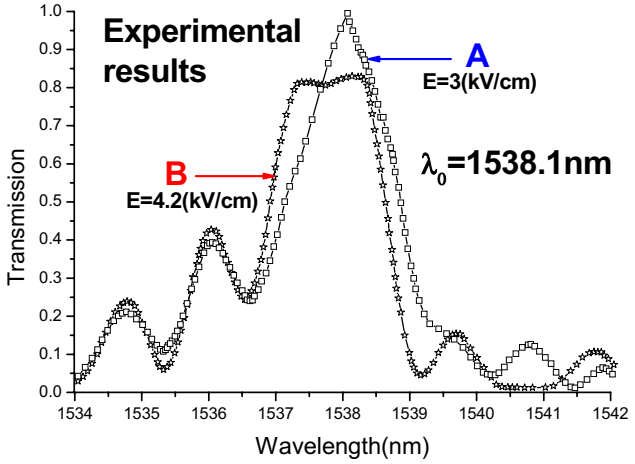

Fig. 11. The transmission spectrums at electric fields of A and B. The curve with square symbol represents the spectrum with 3 (kV/cm) electric field (A) and the curve with star symbol represents the spectrum with 4.2 (kV/cm) electric field (B).

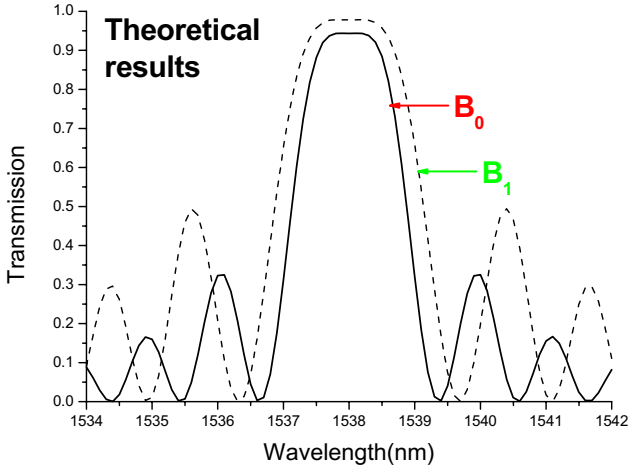

Fig. 12. The theoretical transmission spectrums at critical points B_0 and B_1. The solid curve represents the theoretical spectrum at B_0; The dash curve represents the theoretical spectrum at B_1.

In this section, both the theory and the experiment show that there is a critical voltage at which a flat-top transmission spectrum can be achieved. To have an insight into the flat-top process, more studies should proceed in future. We believe this phenomenon may also be found in other materials and structures similar to PPLN. As the flat-top spectrum is able to keep the signal stable, this finding may improve the possibility of the practical application of Solc-type PPLN filter in optical networks and optical signal processing in future.

2.2.4. *Photovoltaic effect in PPLN crystal*

In the experiments of above sections, we also found that, without field applied, the device also has the function of Solc filter, which shows disagreement with the theory. Our study reveals that the photovoltaic effect (PVE) plays an essential role in the performance of non-field applied PPLN Solc filter.[13] The PVE effect sometimes can not be neglected, especially in electric-optic devices. Our theoretical analysis shows that only the electric field E in the Y direction can enable the Solc filter. If the input polarizer is put in the Y direction, there will be a field formed in the Y direction that will make the device work as a Solc filter; whereas, if the input polarizer is set in the Z direction, no field will cause the half-wave plate rocking and the PPLN will have no filter function. By observing the spectrums with two types of setups shown in Fig. 13, the theoretical analysis is experimentally confirmed in Fig. 14.

On the other hand, this PVE effect inspires us a new thought to build the light controlled optical devices or to measure the PVE coefficients.[14] Figure 15 shows measured output power against wavelength for the PPLN of period 20.8 μm with and without the illumination of the UV light, respectively. The UV light intensity is about 143 mw/cm^2. The passband of the filter moves from 1531.9 nm to 1529.1 nm.4. It costs several seconds until spectrum of the filter becomes stable. However, the peak value and the shape of the pass band are unchanged. It means the y field of the PVE is not changed. This suggests that no y direction field is induced when a non-polarized light propagates in z direction.

2.2.5. *Solc-type filter in Ti:PPLN channel waveguide*

In this section, we will present the latest research on Solc-type filter based on Ti:PPLN channel waveguide which has a significant advantage of low driven voltage. The filtering mechanism of this kind filter is same to the filter based on PPLN crystal introduced above.

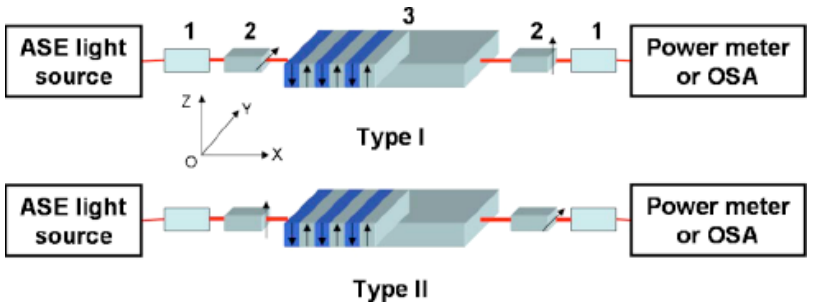

Fig. 13. Two types of device setups for PPLN Solc-type wavelength filter; the arrow on the polarizer indicates the polarization direction. The fact that type I takes on the filter behavior while type II does not reveals the test light has the PVE on the PPLN and it becomes a Solc filter when no external field exists. The numbered components are: 1, collimator; 2, crossed polarizer; 3, PPLN.[13]

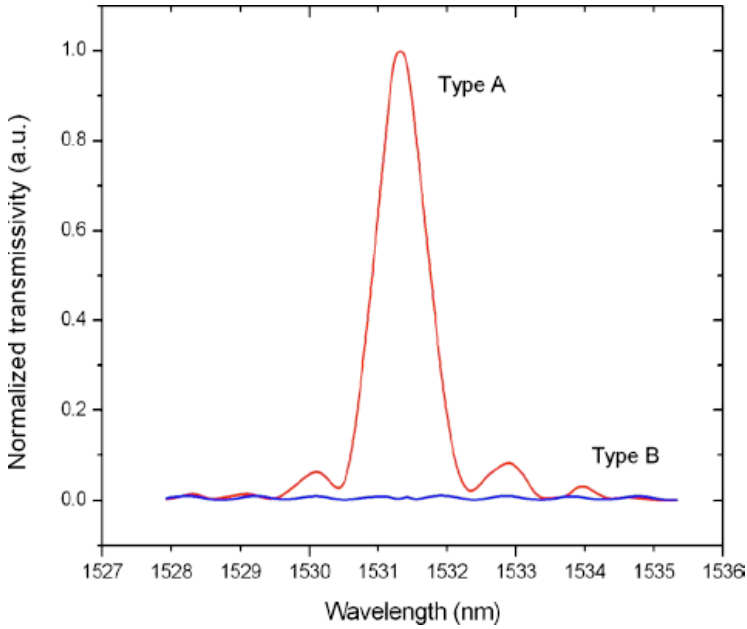

Fig. 14. The transmission curve of the type A setup of device is in accord with the Solc filter function while the type B setup almost has no pass peak.[13]

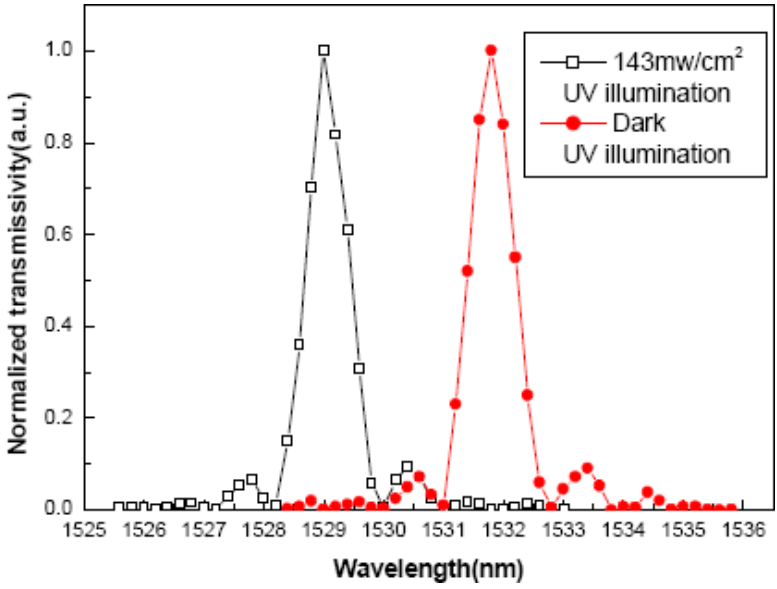

Fig. 15. (Color on line) The spectrum of the PPLN filter under 143 mW/cm^2 UV illumination (empty square symbol) and without UV light illumination (red circle symbol).[14]

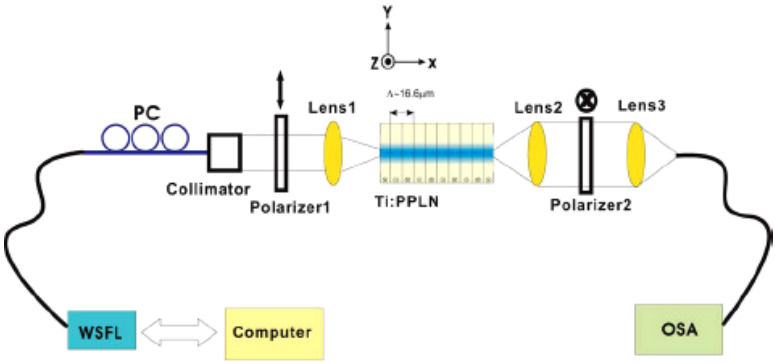

Fig. 16. (Color on line) Experimental setup for the waveguide-type Solc-type filter based on the Ti:PPLN channel waveguide. WSFL, wavelength-swept fiber laser; OSA, optical spectrum analyzer; PC, polarization controller.[15]

In this kind filter, the gap between the electrodes can be as short as (μm) level, therefore, only several voltages are enough for filtering or switching a light.[15] The experimental setup to perform the wavelength filtering based on the Ti:PPLN channel waveguide is shown in Fig. 16. An optical signal from a wavelength-swept fiber laser based on a semiconductor optical amplifier and a Fabry–Perot tunable filter was collimated and end-fire coupled into the Ti:PPLN waveguide, which is placed between two crossed polarizer by a 10× objective lens. The polarization direction of input beam was adjusted parallel to the Y axis of the Ti:PPLN device, and the output signal was observed by an optical spectrum analyzer. The filtering

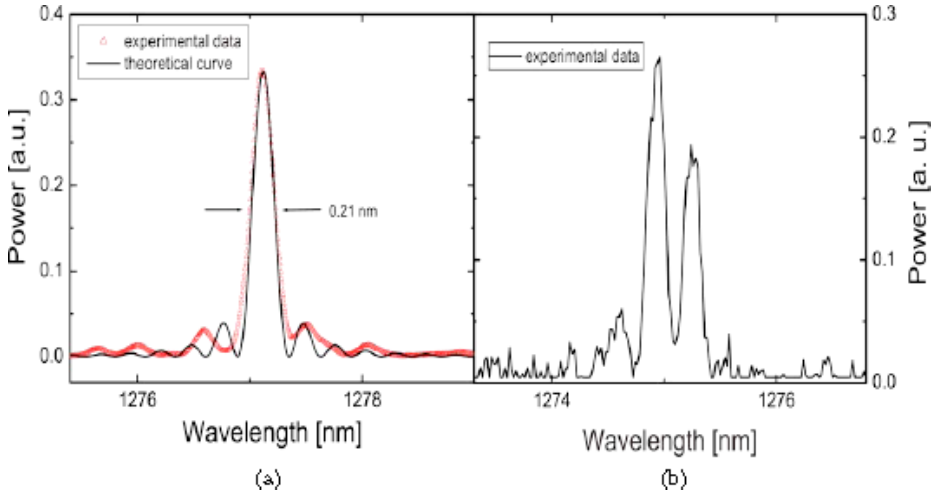

Fig. 17. (Color on line) Optical spectra of the Šolc filter based on the Ti:PPLN waveguide depending on guiding modes at room temperature: (a) one-mode guiding condition, (b) two-mode guiding condition.[15]

results of one-mode guiding condition and two-mode guiding condition are shown in Fig. 17. In one-mode condition, the measured FWHM of the filter was about 0.21 nm, and in two-mode condition, the origin of one peak is the TEM00-like mode, and the other is the TEM01-like mode. The wavelength difference of the two peaks is about 0.8 nm.

Similar to the light controlled optical Solc-type filter by use of PVE effect in PPLN crystal, Lee *et al.* demonstrate a tunable all-optical Solc-type wavelength filter based on Ti:PPLN channel waveguide.[16] Figure 18 shows the centre wavelength of the filter as a function of the UV illumination intensity. As the intensity increases, the centre wavelength of the filter shifts to a shorter wavelength. The measured wavelength tuning rate of the filter was about $-26.42\,\mathrm{nm/W\,cm^{-2}}$ which shows more slant than that of a bulk PPLN Solc-type filter ($-19.23\,\mathrm{nm/W\,cm^{-2}}$).[11] The right axis of Fig. 18 indicates the amount of change in the refractive index difference between n_o and n_e as a function of UV intensity. These results indicate that a Ti:PPLN Solc-type filter gives a wider wavelength tuning range than that of a bulk PPLN Solc-type filter.

3. Polarization Controller

In this section, we will introduce our study on precise linear polarization-state controller based on PPLN,[17] which was also inspired by Lu *et al.'s* study,[4] where they theoretically proposed the electro-optical effect in PPLN. The working mechanism is the same with the Solc-type filter. It is known that with respect to the fundamental wavelength of Solc-type filter, each domain serves as a half-wave plate. Therefore, after passing through the stack of half-wave plates, the optical plane of polarization of the fundamental wavelength rotates continually and emerges finally at an angle of $2N\theta$. As θ is controlled with external electric field, the final rotation angle is as well dominated by the electric field. Consequently, an EO linear

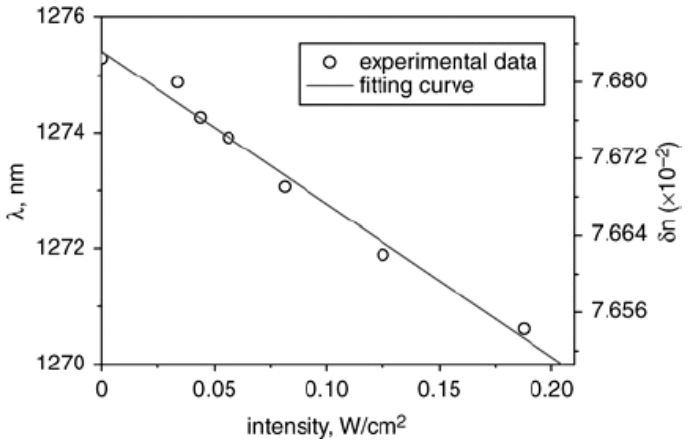

Fig. 18. Centre wavelength of Ti:PPLN Solc-type filter aganst UV illumination intensity.[16]

polarization-state controller for the fundamental wavelength can be realized. In the following discussion, we use another name of "operating wavelength" to represent the fundamental wavelength which is more appropriate than the latter.

As for the PPLN sample employed in the experiment, the operating wavelength is found out to be $\lambda = 1543.47\,\text{nm}$. Then, experimental measurement of the state of polarization of the output light ($\lambda = 1543.47\,\text{nm}$) is shown on a Poincare sphere in Fig. 19 when varying the applied electric field. The experiment shows the state of polarization remains on the equatorial plane when changing the electric field which indicates the output light remains linear state of polarization. The corresponding rotation angle at each electric field is shown in Fig. 20, where the electric field

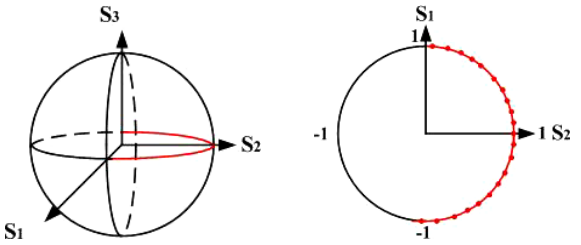

Fig. 19. Experimental measurement of the state of polarization of the output light ($\lambda = 1543.47\,\text{nm}$) on a Poincare sphere when varying the applied electric field from 0 to 3 (kV/cm).[17]

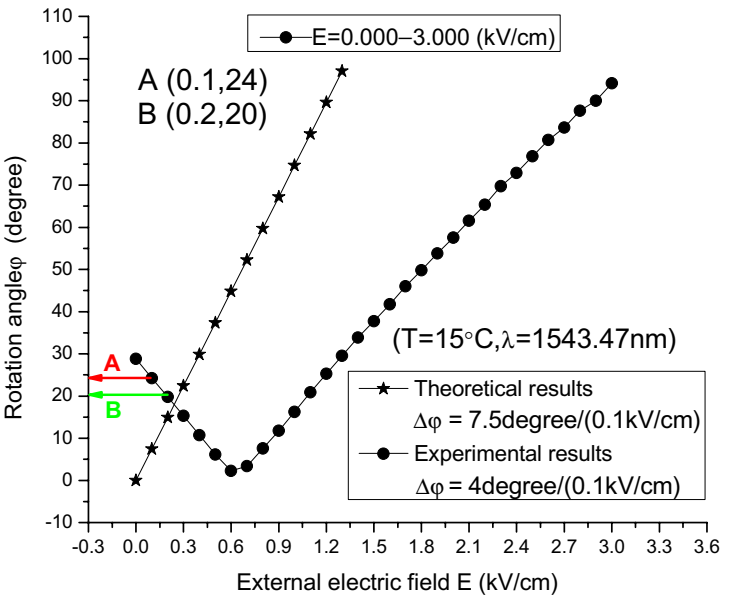

Fig. 20. Experimental measurement of the rotation angle of the output light ($\lambda = 1543.47\,\text{nm}$) when varying the applied electric field from 0 to 3 (kV/cm).[17]

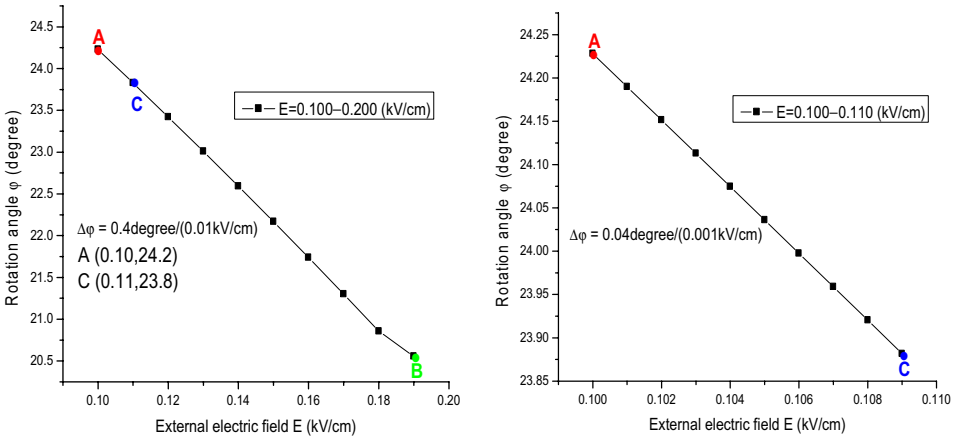

(a) (b)

Fig. 21. Experimental measurement of the rotation angle of the output light ($\lambda = 1543.47$ nm) when varying the applied electric field with smaller step. (a) The external electric field varies from 0.100 to 0.200 (kV/cm); (b) The external electric field varies from 0.100 to 0.110 (kV/cm).[17]

intensity is tuned from 0 to 3 (kV/cm), with the step of 0.1 (kV/cm) each time and the rotation angle linearly varies between 0–100 degrees.

To obtain higher precision, we reduce the electric field step to 0.01 (kV/cm) and 0.001 (kV/cm), respectively. Higher precision of 0.4 degree and 0.04 degree is finally achieved, limited by the accuracy of the measurement system, which are shown in Fig. 21. Moreover, the operating wavelength can be tuned to a series of different wavelengths by changing the temperature.

The device operating as a precise linear polarization-state controller may find many applications where high precision control of linear polarization-state light is requested ranging from polarization analysis to monitoring of network performance, material birefringence, and measurement of polarization mode dispersion, swept-wavelength measurement, medical imaging and fiber sensor systems.

4. Electro-Optical Switch

High speed optical switch is one of the key components in optical communication. In this section, with the same experimental setup of Solc-type filter, we change to with focus on the application of a precise EO switch. The first observation of an EO switch in PPLN is shown in Fig. 22, where high extinction ratio with 43 dB is gained in the experiment.

However, an obstacle to the application of such switch is the narrowband and wavelength limit. Inspired by the discovery of flat-top spectrum in PPLN in 2.2.3 section, we further find out a critical electric field at which the spectrum evolves into broadband. Figure 23 shows the flat-top width and the critical electric field as a function of the domain number. Considering a given PPLN with 60 domains, the

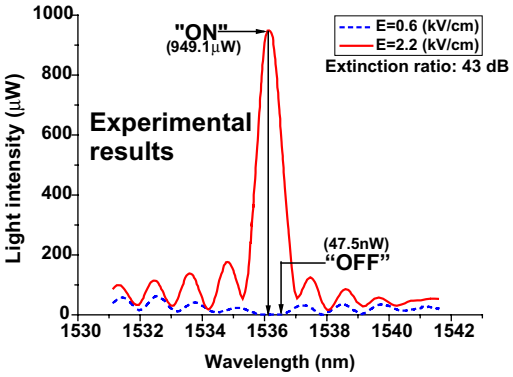

Fig. 22. The experimental transmission spectrums at electric fields of 2.2 (kV/cm) and 0.6 (kV/cm); The solid curve represents the switching state "ON", and the dash curve represents the state "OFF".

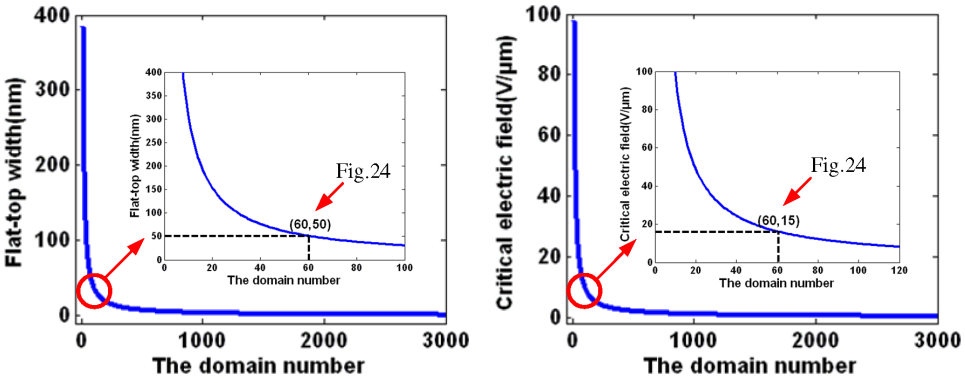

(a) (b)

Fig. 23. (a) The flat-top width as a function of the domain number; (b) The critical electric field as a function of the domain number; The transmission spectrum at the domain number of 60 is showed in Fig. 24.

transmission spectrum at the critical electric field is shown in Fig. 24, which has a broadband with 50 nm flat-top width. The broadband here can efficiently extend the switch's operating wavelengths. However, although sharp increase of the flat-top width can be learned from Fig. 23(a), higher width than 50 nm is impossible in practice, because the corresponding critical electric field will synchronously rapidly rise in Fig. 23(b), which will damage the PPLN.

5. Laser Q-Switch

A class of Q-switched lasers employs a fast intra-cavity polarization rotator for switching the laser polarization between high- and low-loss laser modes. The two

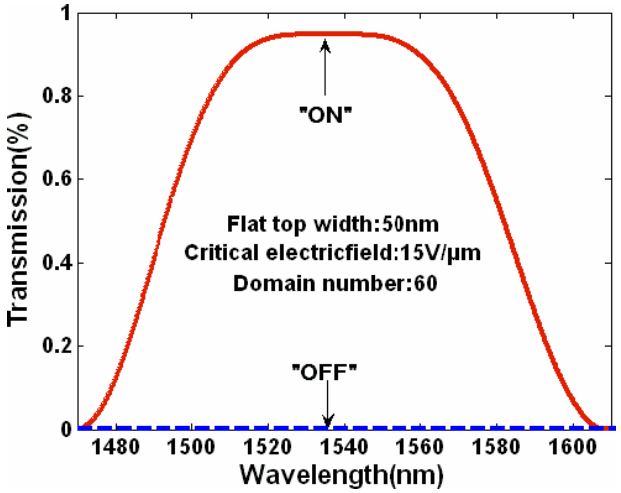

Fig. 24. The transmission spectrum at the critical electric field of 15 (V/μm) when the domain number is 60.

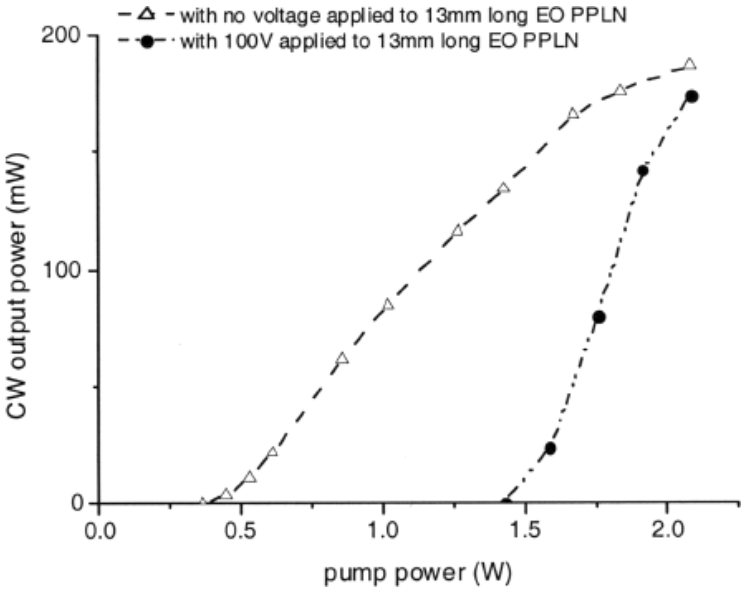

Fig. 25. CW performance of the Nd:YVO4 laser with (solid curve) and without (dashed curve) a 100-V voltage applied to the EO PPLN. With the 100-V voltage, the laser threshold was increased from 400 mW to 1.4 W because of the polarization-rotation effect from the EO PPLN crystal.[18]

loss modes can be established by using a polarization-dependent loss element such as EO PPLN crystal. In this section, we present another significant application on laser Q switch laser based on EO PPLN crystal, which were proposed by Chen *et al.*[18] and Lin *et al.*[19]

In the year of 2003, Chen *et al.* successfully employed a PPLN Pockels cell as a laser Q-switch with a switching voltage as low as ∼100 V.[18] The PPLN Pockels cell consists of a quarter-wave plate and an EO PPLN crystal having the same crystal orientation as a typical PPLN wavelength converter.

Figure 4 shows the continuous-wave (CW) performance of the Nd:YVO4 laser with and without a 100-V voltage applied to the EO PPLN crystal. Without the applied voltage, the Nd:YVO4 laser had a CW threshold of 400-mW pump power, attributable to the high output coupling loss (13%). With a 100-V voltage applied to the EO PPLN crystal, the laser's CW threshold was increased to ∼1.4-W pump power as expected from the polarization rotation effect.

To show laser Q-switching operation, the EO PPLN is drove by using a 7-kHz, 100-V voltage pulser with a 300-ns pulse width. At 1.2-W pump power, 60-mW average power or 0.74-kW peak power with 8.6-mJ pulse energy in an 11.6-ns laser pulse width is measured in the experiment (Fig. 26).

Despite the low switching voltage and excellent integrated QPM performance, the PPLN Pockels cell was sensitive to temperature and generated appreciable green-laser power at 532 nm in the Nd:YVO4 laser, both due to the QPM structure in the PPLN. It is desirable to have a "green-free" and temperature-insensitive laser Q-switch that still retains the advantages of low switching voltage and excellent integrated QPM performance. In the year of 2007, Lin *et al.* reported such a laser Q-switch which had overcome the previous disadvantages using a novel EO PPLN Bragg modulator, producing 7.8 ns, 201 μJ pulses at a 10 kHz repetition rate when

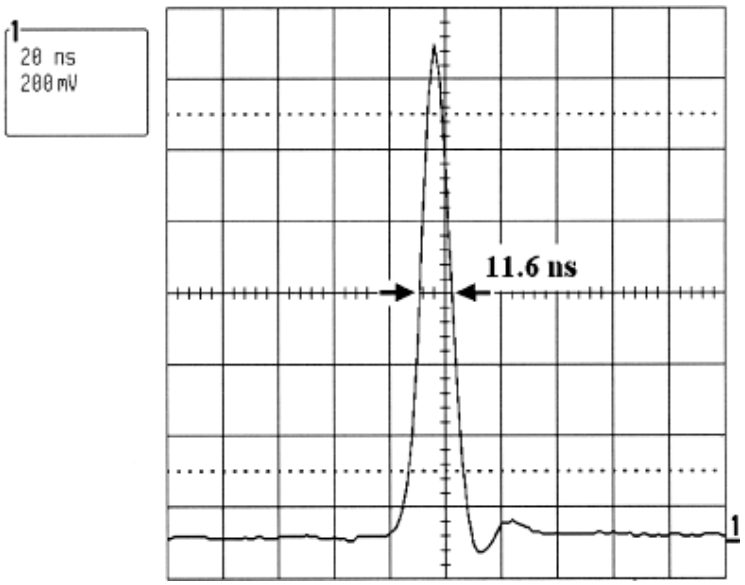

Fig. 26. Measured Q-switched pulse from the EO PPLN Q-switched Nd:YVO4 laser at 1.2-W pump power. The pulse width was 11.6 ns, and the peak power was ∼0.74 kW.[18]

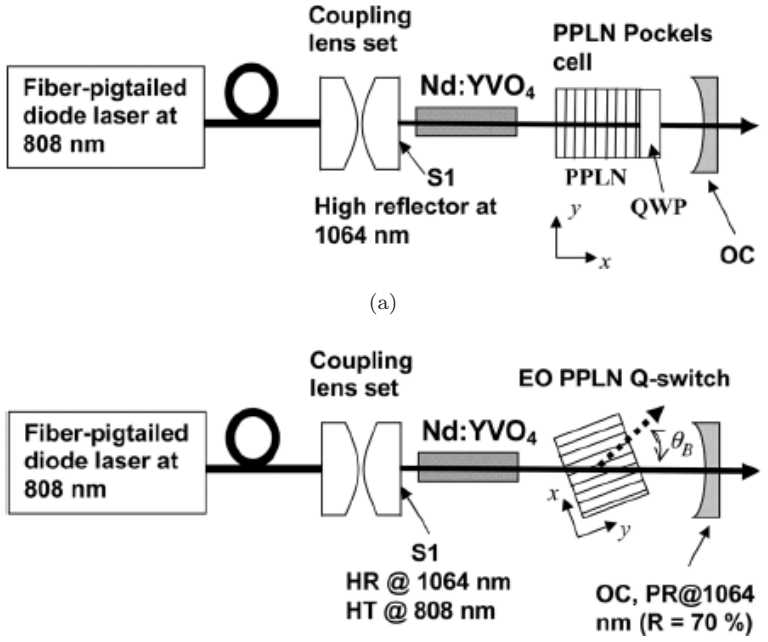

Fig. 27. Schematic of the actively Q-switched Nd:YVO4 laser using (a) a PPLN Pockels cell and (b) an EO PPLN Bragg modulator as a laser Q-switch. The laser cavity is formed by the surface S1 and the output coupler (OC). In (b), the Bragg angle θ_B is exaggerated for clarity. QWP, quarter-wave plate; HR, high reflection; HT, high transmission; PR, partial reflection.[19]

pumped by a 19.35 W diode laser at 808 nm.[19] The schematic setups of two different kind laser Q-switches are shown in Fig. 27.

Figure 28 shows the measured Q-switched pulse energy versus the diode pump power of the second kind laser Q-switch. At 19.35 W pump power, the Q-switched output pulse at 1064 nm has 201 μJ energy and 7.8 ns width, corresponding to a peak power of 26 kW. The error bar in the plot shows that the pulse-to-pulse energy jitter was less than 5% over the range of our measurement. The inset shows the temporal profile of the Q-switched output pulse. In the experiment, no noticeable change was observed on the laser performance when the EO PPLN grating was heated from room temperature to 180°C; In addition, no green-laser power produced from the non-phase-matched second-harmonic generation in the EO PPLN grating was observed in the experiment as well. The experiment successfully confirmed the advantages of this kind Q-switch.

6. Conclusion

In this paper, we have reviewed essential applications by use of polarization coupling in periodically poled lithium niobate during the past five years. Because of

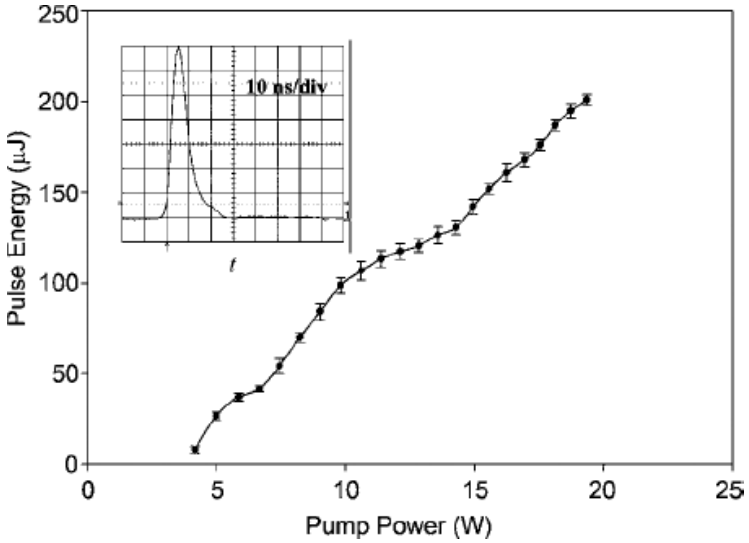

Fig. 28. Output pulse energy of the actively Q-switched Nd:YVO4 laser versus pump power. With 19.35 W pump power at 808 nm, the 1064 nm laser pulse has an energy of 201 $\sim$ J and a width of 7.8 ns, corresponding to a laser peak power of 26 kW. The inset shows the measured temporal profile of the Q-switched laser pulse.[19]

the outstanding properties of PPLN, we believe that PPLN will remain to be an important contemporary realm of science.

References

1. G. A. Magel, M. M. Fejer and R. L. Byer, Quasi-phase-matched second-harmonic generation of blue light in periodically poled $LiNbO_3$, *Appl. Phys. Lett.* **56** (1990) 108–110.
2. C. Q. Xu, H. Okayama and M. Kawahara, 1.5 μm band efficient broadband wavelength conversion by difference frequency generation in a periodically domain-inverted $LiNbO_3$ channel waveguide, *Appl. Phys. Lett.* **63** (1993) 3559–3561.
3. J. J. Zheng, Y. Q. Lu, G. P. Luo, J. Ma, Y. L. Lu, N. B. Ming, J. L. He and Z. Y. Xu, Visible dual-wavelength light generation in optical superlattice through Er:$LiNbO_3$ unconversion and quasi-phase-matched frequency doubling, *Appl. Phys. Lett.* **72** (1998) 1808–1810.
4. Y. Q. Lu, Z. L. Wan, Q. Wang, Y. X. Xi and N. B. Ming, Electro-optic effect of periodically poled optical superlattice $LiNbO_3$ and its applications, *Appl. Phys. Lett.* **77** (2000) 3719.
5. X. F. Chen, J. H. Shi, Y. P. Chen, Y. M. Zhu, Y. X. Xia and Y. L. Chen, Electro-optic Solc-type wavelength filter in periodically poled lithium niobate, *Opt. Lett.* **28** (2003) 2115–2117.
6. D. H. Jundt, Temperature-dependent Sellmeier equation for the index of refraction, no, in congruente lithium niobate, *Opt. Lett.* **22** (1997) 1553–1555.
7. Y. M. Zhu, X. F. Chen, J. H. Shi, Y. P. Chen, Y. X. Xia and Y. L. Chen, Wide-range tunable wavelength filter in periodically poled lithium niobate, *Opt. Comm.* **228** (2003) 139–143.

8. J. H. Wang, J. H. Shi, Z. E. Zhou and X. F. Chen, Tunable multi-wavelength filter in periodically poled LiNbO3 by a local-temperature-control technique, *Opt. Exp.* **15** (2007) 1561.
9. X. Gu, X. F. Chen, Y. P. Chen, X. L. Zeng, Y. X. Xia and Y. L. Chen, Narrowband multiple wavelengths filter in aperiodic optical superlattice, *Opt. Commun.* **237** (2004) 53–58.
10. A. Yariv and P. Yeh, *Optical Waves in Crystal: Propagation and Control of Laser Radiation* (Wiley, NewYork, 1984).
11. C. H. Lin, Y. H. Chen, S. W. Lin, C. L. Chang, Y. C. Huang and J. Y. Chang, Electro-optic narrowband multi-wavelength filter in aperiodically poled lithium niobate, *Opt. Exp.* **15** (2007) 9859–9866.
12. K. Liu, J. H. Shi, Z. E. Zhou and X. F. Chen, Electro-optic Solc-type flat-top bandpass filter based on periodically poled lithium niobate, *Opt. Commun.* **282** (2009) 1207–1211.
13. L. J. Chen, J. H. Shi, X. F. Chen and Y. X. Xia, Photovoltaic effect in a periodically poled lithium niobate Solc-type wavelength filter, *Appl. Phys. Lett.* **88** (2006) 121118.
14. J. H. Shi, J. H. Wang, L. J. Chen, X. F. Chen and Y. X. Xia, Tunable Šolc-type filter in periodically poled LiNbO3 by UV-light illumination, *Opt. Exp.* **14** (2006) 6279.
15. Y. L. Lee, N. E. Yu, C.-S. Kee, D.-K. Ko, J. Lee, B.-A. Yu, W. Shin, T. J. Eom and Y.-C. Noh, Wavelength filtering characteristics of Solc filter based on Ti:PPLN channel waveguide, *Opt. Lett.* **32** (2007) 2813–2815.
16. Y. L. Lee, N. E. Yu, C.-S. Kee, D.-K. Ko, Y.-C. Noh, B.-A. Yu, W. Shin, T.-J. Eom, K. Oh and J. Lee, All-optical wavelength tuning in Solc filter based on Ti:PPLN waveguide, *Electron. Lett.* **44** (2008) 30–32.
17. K. Liu, J. H. Shi and X. F. Chen, Linear polarization-state generator with high precision in periodically poled lithium niobate, *Appl. Phys. Lett.* **94** (2009) 101106.
18. Y. H. Chen and Y. C. Huang, Actively Q-switched Nd:YVO4 laser using an electro-optic periodically poled lithium niobate crystal as a laser Q-switch, *Opt. Lett.* **28** (2003) 1460–1462.
19. Y. Y. Lin, S. T. Lin, G. W. Chang, A. C. Chiang, Y. C. Huang and Y. H. Chen, Electro-optic periodically poled lithium niobate Bragg modulator as a laser Q-switch, *Opt. Lett.* **32** (2007) 545–547.